Atlantis Highlights in Material Sciences and Technology (AHMST), volume 1
International Symposium "Engineering and Earth Sciences: Applied and Fundamental Research" (ISEES 2019)

Phasing Diagrams of $TlInSe_2$ - $CuInSe_2$ and $TlInSe_2$ - $AgInSe_2$ Systems

Matiev A.Kh.
Department of general physics
Ingush State University
Magas, Russia
Department of physics
Grozny State Petroleum Technical University
named after M.D. Millionschikov
Grozny, Russia
matiyev-akhmet@yandex.ru

Uspazhiev R.T.
Department of physics
Grozny State Petroleum Technical University
named after M.D. Millionschikov
Grozny, Russia
Department of material sciences
Kh. Ibragimov Complex Institute of the Russian Academy of Sciences
Grozny, Russia
russlan-chr@mail.ru

Khamkhoev V.M.
Department of general physics
Ingush State University
Magas, Russia
khamkhoev1950@mail.ru

Gachaev A.M.
Department of advanced and applied mathematics
Grozny State Petroleum Technical University
named after M.D. Millionschikov
Grozny, Russia
Department of physical and mathematical research
Kh. Ibragimov Complex Institute of the Russian Academy of Sciences
Grozny, Russia
gachaev_chr@mail.ru

Evloev A.V.
Department of general physics
Ingush State University
Rostov, Russia
evlihan@mail.ru

Evtieva R.M.
Department of physics
Grozny State Petroleum Technical University named after M.D. Millionschikov
Grozny, Russia
roza.efteeva@mail.ru

Israilova L.I.
Department of physics
Grozny State Petroleum Technical University named after M.D. Millionschikov
Grozny, Russia
daydov.akhmed.1997@mail.ru

Gasanov N.Z.
"Crystallophysics" laboratory
Institute of physics of national academy of sciences of Azerbaidzhan
Baku, Azerbaidzhan
nazim_gasanov@mail.ru

***Abstract* – Phase equilibrium was studied on the basis of the data of differential thermal, X-ray phase analyzes, as well as measurements of conductivity and density. Phasing diagrams of $TlInSe_2$-$CuInSe_2$ and $TlInSe_2$-$AgInSe_2$ systems were constructed over the entire concentration range. The studied systems were quasi-binary with limited mutual solubility of the components in the solid state. State diagrams were eutectic in nature. The areas of mutual solubility at eutectic temperatures were approximately 3 mol. % on each side in the $TlInSe_2$ system - $CuInSe_2$ and 15 mol. % on the basis of $TlInSe_2$ and 5 mol. % based on $AgInSe_2$ in the $TlInSe_2$ - $AgInSe_2$ system. The solid solutions based on $CuInSe_2$ and $AgInSe_2$, as well as the initial compounds themselves, undergo phase transformations from the chalcopyrite structure to the sphalerite structure. It was found that in these systems limited solid solutions were formed, which were 2.5 mol. % at indoor temperature from $TlInSe_2$ and 1.5 mol. % on $CuInSe_2$ in the $TlInSe_2$-$CuInSe_2$ system and 3 mol. % on $TlInSe_2$, 2 mol. % on $AgInSe_2$ in the $TlInSe_2$-AgInSe system.**

Keywords – diagram; solid solution; smolidus; liquidus; X-ray analysis; electrical conductivity; density.

I. INTRODUCTION

The $TlInSe_2$, $CuInSe_2$ and $AgInSe_2$ compounds, which belong to new classes of semiconductors of the type $A^{III}B^{III}C_2^{VI}$ and $A^{I}B^{III}C_2^{VI}$ are of scientific interest for modern

optoelectronics and is currently being intensively studied [1-11, 15].

$TlInSe_2$ - is a typical representative of recently discovered non polyvalent semiconductor compounds, which, like its other crystal chemical analogues which belong to the above mentioned class, has a specific structural feature of the crystal lattice composed of two independent structural units — an octahedron with monovalent thallium ions and a tetrahedron with trivalent ions indium surrounded by four selenium atoms with a covalent-tetrahedral bond [1]. The $CuInSe_2$ and $AgInSe_2$ compounds crystallize into a chalcopyrite structure, in which two types of cathinones forming an ordered sublattice. A unit cell containing 8 atoms (2Cu, 2In, 4Se) is characterized by the presence of a volume center and an axis ratio close to 2 [1].

The purpose of this article is to study the interaction in the $TlInSe_2$ - $CuInSe_2$ and $TlInSe_2$ - $AgInSe_2$ systems over the entire concentration range.

II. METHODS AND MATERIALS

In order to construct the $TlInSe_2$ - $CuInSe_2$ and $TlInSe_2$ - $AgInSe_2$ phasing diagram of system, the authors synthesized $TlInSe_2$ and $CuInSe_2$ and $AgInSe_2$ ternary semiconductor compounds. The starting materials were high purity elements: Tl-000; Cu-OCCH-11-4; Se — OSCl-17-4; In-000; Ag-OCCH-4-11-4. The oxide film and other contaminants were removed from the copper surface by etching in a 5% HNO_3 solution for 8–10 minutes, followed by washing in running distilled water, and thallium was subjected to vacuum distillation. The ampoules for synthesis made of thick-walled quartz with an internal diameter of 25 mm were first etched with 40% HF solution for 5 minutes, washed intensively with distilled water, and then annealed in a vacuum oven at a temperature of 1300K.

In order to prevent the melting contact with the surface of quartz, the inner part of the ampoules was covered with a layer of graphite. The starting compounds were obtained by direct fusion of the components, taken in a stoichiometric ratio, in the evacuated to a residual pressure of 1.10–3 Pa of quartz ampoules.

The synthesis was carried out in two-section heaters at a temperature of 1300 K for $CuInSe_2$, 1100 K for $AgInSe_2$ and 1100 K for $TlInSe_2$. The $TlInSe_2$ and $CuInSe_2$ and $AgInSe_2$ melts were exposed to these temperatures for 4 hours, subjecting to intensive mixing, and then the temperature was slowly lowered to 750K and 800K, respectively. In order to bring the alloys to an equilibrium state, homogenizing annealing was used at the indicated temperatures for 240 hours. The single phase and homogeneity of the obtained compounds were controlled by the methods of differential thermal (DTA) and X-ray phase (XRA) analysis.

According to the phasing diagrams, only the $TlInSe_2$, $CuInSe_2$ or $AgInSe_2$ lines appeared on the X-ray patterns of the alloys (Fig. 2, 6, d, e). The areas of existence of solid solutions at indoor temperature were: 2.5 mol. % on $TlInSe_2$ and 1.5 mol. % on $CuInSe_2$ in the $TlInSe_2$ - $CuInSe_2$ system and 3 mol. % on $TlInSe_2$ and 2 mol. % on $AgInSe_2$ in the $TlInSe_2$ - $AgInSe_2$ system.

Thus, the radiographs of alloys of solid solutions did not differ from radiographs of the starting compounds. The presented phasing diagrams can be attributed to type of VI transformations of solid solutions according to Roozeboom [13].

Using the above mentioned method 6 g four-component samples were prepared from the obtained compounds.

DTA was carried out using a software device for the increase and decrease in temperature [12], a two-coordinate recorder H-306 and a highly sensitive two-stage amplifier assembled on the basis of integrated circuits K140UD13 and K140UD6. DTA curves of alloys were removed at a heating rate of ≈ 10 ° C / min. using Pt-Pt / Rh thermocouples PR-30/6, graduated by melting temperature of the following substances: Bi, Pb, Se, Te, Sb, KCl, NaCl, Na2SO4, Ag and Cu. The error in the determination of the temperature was 50 ° C. One-gram samples were evacuated in Stepanov quartz vessels with an internal diameter of 5 mm, and annealed alumina was used as a reference.

Resistance was measured using universal voltmeters Shch31, B7-30 (the error did not exceed 0.05% in the first case and 5% in the second). The substance in the form of a fine mass was pressed into quartz capillaries with a length of 10 mm and a diameter of 2.7 mm. The intrinsic resistance of the capillaries exceeded 10^{18} Ohms, which guaranteed the absence of a shunt effect on measurements, even for high-resistance samples on $TlInSe_2$. The frontal segments of the capillaries were covered with indium, into which copper electrodes were introduced.

X-ray phase analysis of the system was performed on the installation of Dron-3 (CuKα - Ni radiation - filter, 40 kV, 20 mA, the speed of movement of the counter was 1º / min. The sample in the form of powder was rotated during the shooting.

III. RESULTS

The phasing diagrams of the $Tl_{1-x}Cu_xInSe_2$ and $Tl_{1-x}Ag_xInSe_2$ systems, based on the results of DTA, XRA, and also on measurements of specific electrical conductivity and pycnometric density, are presented in Figure 1.2. The studied systems are quasi-binary with limited mutual solubility of the components in the solid state. Phasing diagrams are eutectic in nature. The coordinates of the eutectic points were specified by Tamman building triangles. The temperature of the $AgInSe_2$ ordering is 11 degrees lower than the melting temperature (for a visual demonstration it is shifted somewhat down in Figure 2). According to the obtained data, the temperature of ordering was 1045 K, which complies with the results of the research works [1, 5–9]).

The solid solutions based on $CuInSe_2$ and $AgInSe_2$, like the initial compounds themselves, undergo phase transformations and chalcopyrite structures into the sphalerite structure. According to the obtained data, the temperature of the phase transition (temperature of ordering) in $CuInSe_2$ was 1083 K, which also complies with the results of the research works [1, 8, 9]. Melting points $CuInSe_2$ and $AgInSe_2$ were 1263K and 1056K, respectively.

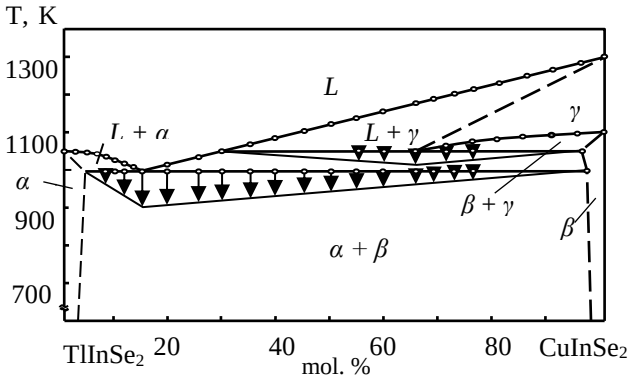

Fig. 1. System phasing diagram $TlInSe_2$ -

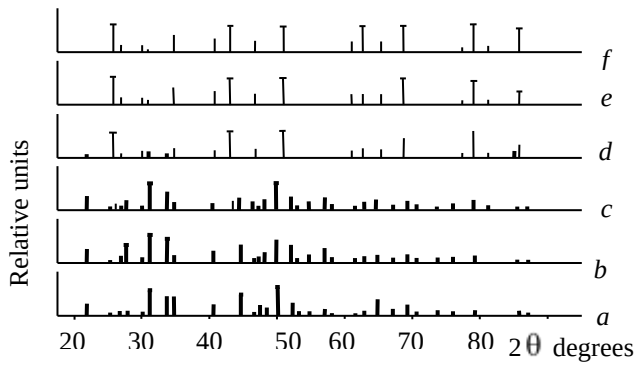

Fig. 2. System bar charts $TlInSe_2$ - $CuInSe_2$:
a - TlInSe2; *b*- $Tl_{0.98}Cu_{0.02}InSe_2$; *c* - $Tl_{0.97}Cu_{0.03}InSe_2$;
d- $Tl_{0.02}Cu_{0.98}InSe_2$; e - $Tl_{0.01}Cu_{0.99}InSe_2$; *e* - $CuInSe_2$.

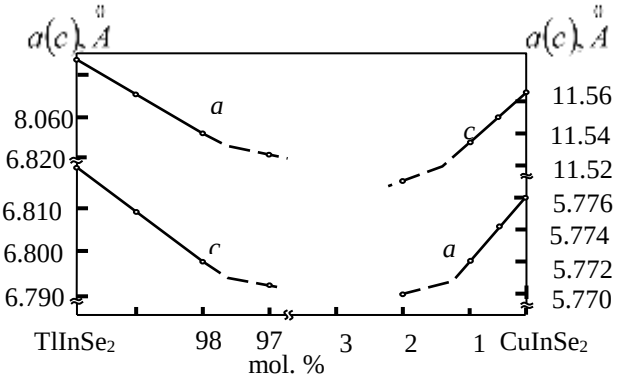

Fig. 3. Dependence of changes in tetragonal parameters cells by composition in the system $TlInSe_2$ - $CuInSe_2$.

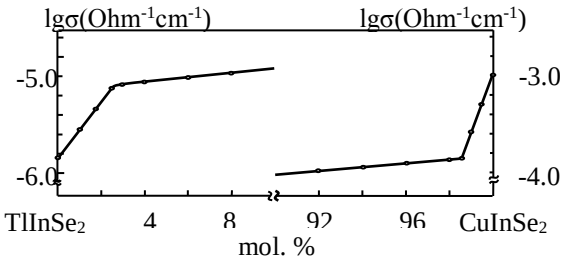

Fig.4. Dependence of specific conductivity on composition in the system $TlInSe_2$ - $CuInSe_2$.

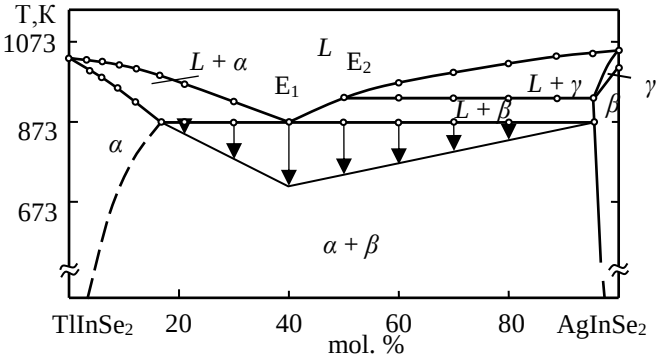

Fig. 5. System phasing diagram TlInSe2 -

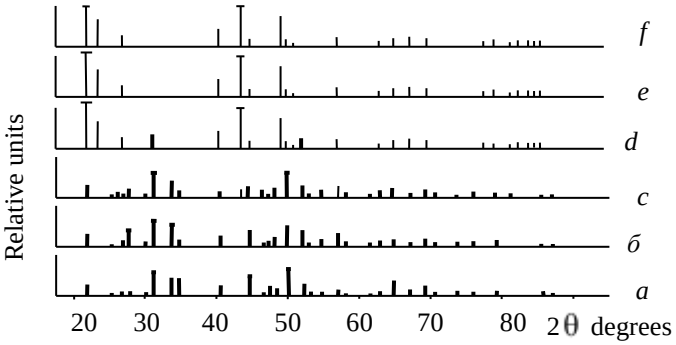

Fig. 6. System bar charts $TlInSe_2$ - $AgInSe_2$:
a - $TlInSe_2$; *b* - $Tl_{0.975}Ag_{0.025}InSe_2$; *c*- $Tl_{0.97}Ag_{0.03}InSe_2$;
d - $Tl_{0.03}Ag_{0.97}InSe_2$; *e* - $Tl_{0.02}Ag_{0.98}InSe_2$; *f* - $AgInSe_2$.

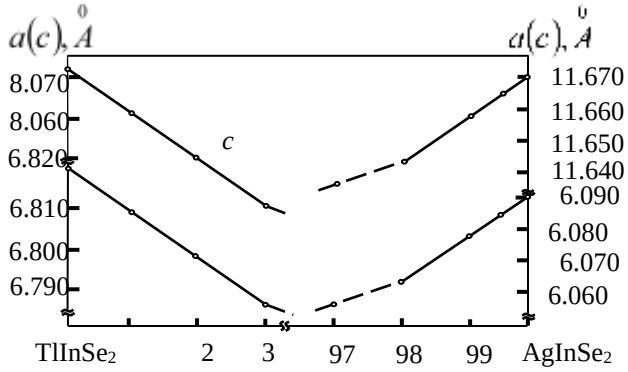

Fig. 7. Dependence of changes in tetragonal parameters cells by composition in the system $TlInSe_2$ - $AgInSe_2$.

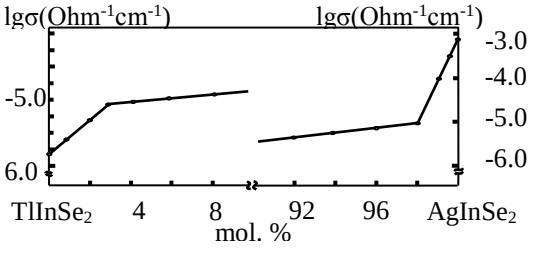

Fig.8. Dependence of specific conductivity on composition in the system $TlInSe_2$ - $AgInSe_2$.

According to the phasing diagrams, only the $TlInSe_2$, $CuInSe_2$ or $AgInSe_2$ lines appeared on the X-ray patterns of the alloys (Fig. 2, 6, d, e). The areas of existence of solid solutions at indoor temperature were: 2.5 mol. % on $TlInSe_2$ and 1.5 mol. % on $CuInSe_2$ in the $TlInSe_2$ - $CuInSe_2$ system and 3 mol. % on $TlInSe_2$ and 2 mol. % on $AgInSe_2$ in the $TlInSe_2$ - $AgInSe_2$ system.

Thus, the radiographs of alloys of solid solutions did not differ from radiographs of the starting compounds. The presented phasing diagrams can be attributed to type of VI transformations of solid solutions according to Roozeboom [13].

Figure 3, 7 show the concentration dependences of the parameters of tetragonal cells in the $TlInSe_2$ – $CuInSe_2$ and $TlInSe_2$ – $AgInSe_2$ systems. In the area of 97.5 –100 mol. % $TlInSe_2$ and 98.5 - 100 mol. % $CuInSe_2$, as well as in the area of 97-100 mol. % $TlInSe_2$ and 98.5 - 100 mol. % $AgInSe_2$, the lattice parameters are additively reduced.

TABLE I. DENSITY IN THE SYSTEMS OF $Tl_{1-x}Cu_xInSe_2$ AND $Tl_{1-x}Ag_xInSe_2$

Compound	X-ray density, g/cm^3	Pycnometric density, g/cm^3
$TlInSe_2$	7.082	7.080
$Tl_{0.99}Cu_{0.01}InSe_2$	7.086	7.084
$Tl_{0.98}Cu_{0.02}InSe_2$	7.095	7.093
$Tl_{0.97}Cu_{0.03}InSe_2$	7.096	7.094
$Tl_{0.99}Ag_{0.01}InSe_2$	7.090	7.089
$Tl_{0.98}Ag_{0.02}InSe_2$	7.101	7.099
$Tl_{0.975}Ag_{0.03}InSe_2$	7.112	7.110
$Tl_{0.96}Ag_{0.04}InSe_2$	7.114	7.113
$CuInSe_2$	5.750	5,749
$Tl_{0.005}Cu_{0.995}InSe_2$	5.770	5.772
$Tl_{0.01}Cu_{0.99}InSe_2$	5.795	5.791
$Tl_{0.02}Cu_{0.98}InSe_2$	5.800	5.798
$AgInSe_2$	5.840	5.838
$Tl_{0.005}Ag_{0.995}InSe_2$	5.860	5.857
$Tl_{0.01}Ag_{0.99}InSe_2$	5.890	5.888
$Tl_{0.025}Ag_{0.98}InSe_2$	5.910	5.907
$Tl_{0.03}Ag_{0.97}InSe_2$	5.920	5.910

Conductivity concentration dependencies (Fig. 4, 8) do not contradict the presented phasing diagrams and form characteristic bends in the vicinity of the above mentioned limits.

The table presents the values of X-ray pycnometric densities of both the initial compounds and the solid solutions of the systems. The density was determined using a pycnometer. Toluene was used as a pycnometric liquid. Since the values of densities according to XRA data coincide within the error with the experimentally found ones, the studied solid solutions can be attributed to substitutional solid solution [14]. From the analysis of tabular data it can be seen that at the limits of mutual solubility, the value of densities reveal characteristic behavior.

IV. CONCLUSION

1. These compounds form limited solid solutions (type VI according to Rooseboom): 2.5 mol. % on the $TlInSe_2$ and up to 1.5 mol. % on the $CuInSe_2$ in the $TlInSe_2$-$CuInSe_2$ system and 3 mol. % on $TlInSe_2$ and 2 mol. % on $AgInSe_2$ in the $TlInSe_2$-$AgInSe_2$ system at indoor temperature.
2. The mutual solubility of the initial components in the studied systems increases during the transition from copper atoms Cu to silver atoms Ag, which is apparently reasoned by a decrease in the difference in the ionic radii of thallium and silver.

References

[1] A.Kh. Matiev, Phase equilibria and electron-optical properties of T1B3C62-A1B3C62 systems (A-Cu, Ag; B-Iп, Ga; C-S, Se2). PhD thesis on Physics and Mathematics Sciences, UlSU, 2005, 399 p.

[2] S.N. Mustafaeva, M.M. Asadov, A.I. Jabbarov, "Dielectric properties and charge transfer in TlInSe2) 0.1 (TlGaTe2) 0.9 at direct and alternating current", Solid State Physics, vol. 56, iss. 6, pp. 1055–1059. 2014.

[3] Sh. Hosokawa, J.R. Stellhorn, H. Ikemoto, K. Mimura, K. Wakita, N. Mamedjv, "Lattice Distortions in $TlInSe_2$ Thermoelectric Material Studied X-ray Absorption Fine Structure", Phys. Status Solidi A., pp. 215, 2018.

[4] A.U. Sheleg, V.V. Shevtsova, V.G. Gurtovoy, S.N. Mustafayev, E.M. Kerimov, "Low-temperature X-ray studies of $TlInS_2$, $TlGaS_2$ and $TlGaSe_2$ single crystals", Surface. X-ray, synchrotron and neutron Research, no. 11, pp. 39–42, 2013.

[5] H. Haloui, K.Touafek, M. Zaabat, H. Ben cheikh el hocinem, A. Khelifa, "The Copper Indium Selenium ($CuInSe_2$) thin films solar cells for Hybrid Photovoltaic Thermal Collectors". Energy Procedia, vol. 74, pp. 1213–1219, August 2015.

[6] A.D.P, Leach, J.E. Vacdonald, "Optoelectronic Properties of $CuInS_2$ Nanocrystals and Their Origin", J. Phys. Chem. Lett., no. 7 (3), pp. 572–583, 2016.

[7] S.L. Castro, Sh.G. Bailey, R.P. Raffaella, K.K. Banger, A.F. Hepp, "Synthesis and Characterization of Colloidal $CuInS_2$ Nanoparticles from a Molecular Single-Source Precursor", J. Phys. Chem. B, no. 108 (33), pp. 12429–12435, 2004.

[8] D. Deng, L. Ou, Yu. Gu, "Near-infraed broadly emissive $AgInSe_2$/ZnS quantum dots biomedical optical imaging", J. Of Materials Chemistry C2, no. 34, pp. 7077–7085, 2014.

[9] N. Karunagaran, P. Ramasamy, "Synthesis, growth and characterization of single crystals", Materials Science in Semiconductor Processing, vol. 40, pp. 591–595, December 2015.

[10] G.V. Makhnovets, G.L. Myronchuk, L.V. Piskach, B.V. Vidrynskyi, A.H. Kevshyn, "Study of optical absorption in $TlGaSe_2:Zn^{2+}$ single crystals", Ukr. J. Phys. Opt., vol. 19, iss. 1, pp. 49–59, 2018.

[11] A.T. Nagat, S.E. A. Garni, F.S. Bahabri, G. Attia, S.R. Al Harbi. A.A. Ghamdi, "Electrical and Thermal Transport Properties of $TlGaSe_2$ Single Crystals", JKAU: Sci., vol. 21, no. 1, pp. 13–26, 2009.

[12] V.A. Gavrish, L.F. Illicheva, M.A. Karavanova, A.V. Radkevich, P.E. Stadnik, "Software device to thermostats", Instruments and equipment of the experiment, no. 6, pp. 149–150, 1979.

[13] V.Ya. Anosov, S.A. Pogodin. Basic principles of physical and chemical analysis. Moscow; Leningrad: Publisher AN. THE USSR, 1947.

[14] A.A. Bochvar, Metal Science. Moscow: Metallurgizdat, 1956.

[15] A.Kh. Matiyev, A.V. Yanarsaev, R.T. Uspazhiev, R.M. Efteyeva, "*T–x* Phase Diagram of the $TlGaSe_2$-$AgGaSe_2$ System", Bulletin of the Russian Academy of Sciences. Physics, Inorganic Materials, vol. 51, no. 7, pp. 665–667, 2015.